J Exp Biol Advance Online Articles. First posted online on 1 June 2012 as doi:10.1242/jeb.069245
Access the most recent version at http://jeb.biologists.org/lookup/doi/10.1242/jeb.069245

Mechanisms Contributing to the Dopamine Induction of Crawl-Like Bursting in Leech Motoneurons

Kevin M. Crisp[1]*, Brian R. Gallagher[1], Karen A. Mesce[2]

[1]Biology Department and Neuroscience Program, St. Olaf College, Northfield, MN
[2]Departments of Entomology and Neuroscience, University of Minnesota, Saint Paul, MN

RUNNING HEAD: Dopamine Modulates Leech Motoneurons

*Corresponding author
Kevin M. Crisp, Associate Professor
Biology Dept. and Neuroscience Program
St. Olaf College
1520 St. Olaf Ave.
Northfield, MN 55057
PH: 507-786-3981
FAX: 507-786-3968
crisp@stolaf.edu

SUMMARY

Dopamine (DA) activates fictive crawling behavior in the medicinal leech. To identify the cellular mechanisms underlying this activation at the level of crawl-specific motoneuronal bursting, we targeted potential cAMP-dependent events that are often activated through DA_1-like receptor signaling pathways. We found that isolated ganglia produced crawl-like motoneuron bursting after bath application of phosphodiesterase inhibitors (PDIs) that up-regulated cAMP. This bursting persisted in salines in which calcium ions were replaced with equimolar cobalt or nickel, but was blocked by riluzole, an inhibitor of a persistent sodium current. PDI-induced bursting contained a number of patterned elements that were statistically similar to those observed during DA-induced fictive crawling, except that one motoneuron (CV) exhibited bursting during the contraction rather than the elongation phase of crawling. Although DA and the PDI produced similar bursting profiles, intracellular recordings from motoneurons revealed differences in altered membrane properties. For example, DA lowered motoneuron excitability while the PDI increased resting discharge rates. We suggest that PDIs (and DA) activate a sodium-influx-dependent timing mechanism capable of setting the crawl rhythm and that multiple DA receptor sub-types are involved in shaping and modulating the phase relationships and membrane properties of cell-specific members of the crawl network to generate crawling.

ABBREVIATIONS:

AE	excitor of the subcutaneous annulus erector muscle
AHP	afterhyperpolarization
cAMP	cyclic adenosine monophosphate
CLO	clotrimazole
CPG	central pattern generator
CV	excitor of the ventrolateral circular muscle
DA	dopamine
DCC	discontinuous current clamp
DE-3	dorsal longitudinal muscle excitor
DI-1	dorsal longitudinal muscle inhibitor
DP	dorsal posterior (nerve)
EIA	Enzyme immunoassay
IBMX	3-isobutyl-1-methylxanthine
NS	normal leech saline
PDE	phosphodiesterase
PDI	phosphodiesterase inhibitor
PIR	post-inhibitory rebound
SPL	8-(*p*-suphonyl)theophylline
THP	theophylline
VE-4	ventral longitudinal muscle excitor
VI-2	ventral longitudinal muscle inhibitor

INTRODUCTION

Dopamine (DA) is known to play an impressive and universal role in the control of animal movements, often by exerting prolonged changes in the patterns of activity of locomotor-related neural networks (Chandler and Goldberg, 1984; Flamm and Harris-Warrick, 1986; Kemnitz, 1997; Lapointe et al., 2009; Quinlan et al., 1997; Teyke et al., 1993). In the medicinal leech, for example, DA has been shown to activate the central pattern generator (CPG) underlying crawling behavior (Puhl and Mesce, 2008; Puhl and Mesce, 2010). DA also serves an important function in the selection of competing or incompatible behaviors, exemplified by DA's suppression of swimming activity in the leech (Crisp and Mesce, 2004). Thus, DA often can act as a behavioral switch, both to activate and suppress competing behaviors (Mesce and Pierce-Shimomura, 2010; Vidal-Gadea et al., 2011). This theme of dual regulation appears to be conserved evolutionarily as additional examples can be found across multiple levels of animal complexity; for example, DA released by sensory neurons in *C. elegans* suppresses locomotion so as to prolong grazing when food is available (Sawin et al., 2000) or helps to match locomotor form to either an aquatic or terrestrial environment (Mesce and Pierce-Shimomura, 2010). In the human basal ganglia, DA plays a clinically-relevant role in the focused selection of competing patterns of intended movement (Mink, 1996; Smith et al., 1998), as well as regulating total body movement (e.g., hypokinesia associated with DA deficiency).

That DA can turn on and turn off the operation of competing neural circuits poses a number of fascinating questions, including the cellular mechanisms underlying DA's actions and how individual neurons are modulated in ways that promote or suppress locomotion. The medicinal leech (*Hirudo verbana*) possesses a number of significant advantages for the study of locomotion: it contains many neurons that have been uniquely identified with respect to their morphology, location, characteristic physiological activity, connectivity and behavioral functions (Kristan et al., 2005). Due to these advantages and the accessibility of its nervous system for electrophysiological studies, multiple behaviors in the leech have been analyzed at the level of individual cells, including a cellular-level understanding of behavioral decision-making (Kristan et al., 2005). Because network computational functions and biochemical signaling pathways are remarkably similar to

their vertebrate counterparts (Burrell and Sahley, 2001; Mullins et al., 2011), studies in the leech often have broad instructional value.

In the present study, we set out to understand how DA influences the membrane properties of neurons that might facilitate the production of crawling while suppressing swimming, a competing locomotor behavior. Because it is established that the crawl and swim networks share a number of the same participatory interneurons and motoneurons (Briggman et al., 2005), the issue of how a given neuromodulator can act to bias or facilitate a sub-set of neurons to perform either a crawl or swim pattern is especially compelling. Our study focuses on the larger and more experimentally accessible locomotor-related motoneurons, as a starting point, and the potential roles that DA has on their physiological properties.

MATERIALS AND METHODS

Animals and solutions

Adult medicinal leeches (*Hirudo verbana*) weighing 2-3 g were obtained from Leeches USA Ltd. (Westbury, NY) or Niagara Medicinal Leeches, Inc. (Ontario, Canada) and housed at 10-15ºC in deionized water containing 0.5 g/L Instant Ocean aquarium salts (United Pet Group, Inc.; Cincinnati, OH) with the pH adjusted to 7.4. Leeches were anaesthetized on ice for 10-15 min prior to dissection.

All drugs were obtained from Sigma (Saint Louis, MO) except that the 8(p-sulfophenyl) theophylline (SPT) was obtained from Research Biochemicals, Inc. (Natick, MA). Drugs were dissolved at room temperature in leech saline (Nicholls and Baylor, 1968) containing (in mM): 115 NaCl, 1.8 $CaCl_2$, 4 KCl, 10 Tris-maleate (pH 7.4). IBMX and riluzole were solubilized in DMSO, which was then diluted to the working concentration (0.5 mM) in normal leech saline; the final concentration of DMSO did not exceed 0.1%. Theophylline (THP) was placed in HCl prior to dilution in saline and adjusted to 7.4 pH. The minimal concentration of all solvents was similar to that used previously and shown not to cause physiological effects during drug delivery in leech salines (Crisp and Muller, 2006). During intracellular recordings from motoneurons, 2 mM $MgCl_2$ was added to the saline to reduce DA-induced oscillations, while in other experiments $CaCl_2$ was replaced with equimolar concentrations of $NiCl_2$ or $CoCl_2$.

Electrophysiological recordings

Extracellular recordings of motor neuron DE-3 were obtained by differential recording of the dorsal posterior (DP) nerve. The DP nerve was carefully dissected free from muscle fibers, and a water-tight silicon well was constructed around the cut end of the nerve. Differential recordings were obtained using a model 1700 differential AC amplifier from A-M Systems (Sequim, WA) and filtered using a LPF202A low pass Bessel filter (Warner Instruments, Hamden, CT). Sixty Hz noise and harmonics were eliminated using the Hum Bug Noise Eliminator (Quest Scientific Instruments, Inc. (North Vancouver, BC). Raw data were digitized on a DigiData 132x series analog-to-digital converter from Molecular Devices (Sunnyvale, CA) and recorded using PClamp or AxoScope version 9.2 (Molecular Devices).

Specific neuronal somata were identified by their electrophysiological signature, position in the ganglion, and morphology when filled with label. Intracellular recordings were obtained with an AxoClamp 2B amplifier in bridge or discontinuous current clamp (DCC) mode and with glass microelectrodes (OD 1.0 mm, ID 0.75 mm, borosilicate glass; DAGAN Instruments, Minneapolis, MN) pulled to a tip resistance of 25-30 MΩ on a P-97 microelectrode puller (Sutter Instruments; Novato, CA). Electrodes were filled with 3M K^+ acetate for recordings and with 10 mM Alexa 568 fluorescent label (Invitrogen, Carlsbad, CA) in 200 mM KCl for iontophoretic dye injection. Label was injected into neurons (after re-impalement) for 3-5 min using 500 ms square pulses of -1 nA current. When used for DCC, electrode tips were coated with dimethylpolysiloxane prior to use in order to reduce capacitance. Intracellular filtering and digitizing were as described above for extracellular signals.

cAMP measurements

Enzyme immunoassay (EIA) for measurement of cAMP concentrations were conducted using a cAMP EIA kit from Cayman Chemical (Ann Arbor, MI). Briefly, chains of ganglia from the second to the 20th midbody ganglia inclusive were treated for 30 min at room temperature with 0.5 mM IBMX or drug-free saline. cAMP was then extracted by incubating the leech tissue in 0.1 M HCl for 30 min at room temperature and

analyzed for cAMP concentration according to the manufacturer's instructions. Lysates were analyzed using absorbance in 96-well plates on a plate reader.

Statistical methods and analysis

Parameters and methods used to measure crawl-related burst cycle periods and durations were those of Puhl and Mesce (2008; 2010) and typically involved bursts that had clearly discernable onsets. A minimum of 6-10 consecutive bursts were analyzed for each preparation and means were compared across the number (n) of preparations tested. Standard unpaired Student's *t*-tests and one-way analysis of variance (ANOVA) were conducted, as well as Fisher LSD post-hoc tests, using Statistica version 7.1 (StatSoft Inc; Tulsa, OK). Graphs were generated using SigmaPlot 2004 (Systat Software Inc; Chicago, IL). All statistical tests were two-tailed with a 95% or greater confidence level ($\alpha = 0.05$). Means are reported as ± the standard error of the mean, and were calculated using Microsoft Office Excel 2003 (Microsoft Corporation; Redmond, WA).

RESULTS

Phosphodiesterase inhibitors activate crawl-like bursting in identified motoneurons

While DA has been convincingly demonstrated to activate fictive crawling, even in a single ganglion (Puhl and Mesce, 2008), the subcellular and biochemical mechanisms underlying such activation have yet to be explored. To begin to identify these mechanisms, we sought to determine whether crawling-related activity was dependent on cAMP second-messenger signaling. This approach was taken as the leech CNS is known to possess at least one DA_1-like receptor, which has been shown to be positively coupled to adenylyl cyclase activity (Ali et al., 1998). This activity, in turn, increases the cytoplasmic concentration of cAMP, thus enhancing protein kinase A (PKA) activity and the serine/threonine phosphorylation of cellular proteins, including ion channels possibly involved in neuronal bursting. For example, PKA targets a persistent sodium current to increase bursting in the cerebral giant cells of *Lymnaea* (Nikitin et al., 2006) and increased cAMP levels have been linked to changes in the fictive swimming motor pattern in *Tritonia* (Clemens et al., 2007). Phosphodiesterases (PDEs) are known to inactivate cAMP (thus lowering PKA activity), enabling

phosphatases to dephosphorylate target proteins. Thus, perturbations in cAMP via PDE inhibitors (PDIs) were conducted here to test their contribution towards crawl-related bursting in relevant neurons.

To elevate cAMP levels, we applied the classic PDIs theophylline (THP) and 3-isobutyl-1-methylxanthine (IBMX) while recording from previously identified motoneurons (i.e., DE-3) known to exhibit slow bursting during spontaneous and DA-evoked crawling (Puhl and Mesce, 2008). We observed that 4.4 mM THP applied to individual isolated ganglia induced crawl-like bursting in DE-3 (Fig. 1A) (13 of 15 preparations). However, THP is not only an inhibiter of cytoplasmic PDE activity but an adenosine receptor blocker as well. To control for whether THP might induce crawl-like bursting by blocking adenosine receptors, we used the polar adenosine receptor blocker, 8-(*p*-sulfophenyl) theophylline (SPL; 4.4 mM bath application). [Because of its polarity, SPL mimics the extracellular actions of THP (e.g., adenosine receptor antagonism) but not its intracellular activity (e.g., PDE inhibition).] Blockade of adenosine receptors with SPL was found not to induce rhythmic bursting activity in DE-3 (n = 3; Fig. 1A). Similar to the effects of THP, IBMX (500 µM) produced crawl-like rhythmic bursting in DE-3 (21 of 22 preparations) (Fig. 2A). In Fig. 1B, the cycle periods and burst durations of DE-3 induced by PDIs and by DA were compared using statistical methods. Burst durations and cycle periods were measured and analyzed from a randomly selected subset of ganglia treated with THP (n = 10) and IBMX (n = 10). DE-3 activity during unevoked (i.e., non-pharmacological or sensory induced) fictive crawling was also included in our analyses. Data for the DA and spontaneous fictive crawl studies were originally obtained by Puhl and Mesce (2008); the raw data were reanalyzed here for the quantitative comparisons made. An ANOVA was employed to compare burst durations and cycle periods across all treatments (Fig 1B) There was no statistically significant difference across treatments with respect to cycle period ($F_{4,38} = 0.71$; $p = 0.5$), but the effect of treatment on burst duration was statistically significant ($F_{4,38} = 5.07$; $p < 0.01$). Post-hoc Fisher LSD tests showed no statistically significant differences between burst durations obtained from single ganglia treated with DA (n = 10), THP (n = 10), IBMX (n = 10), or from intact (i.e., whole) leech nerve cords (n = 10) that exhibited spontaneous fictive crawling in normal saline (NS) in the absence of DA (CNS in NS; n = 10; Fig. 1B). Only

the IK channel blocker clotrimazole (CLO, discussed in more detail later) resulted in a significantly longer burst duration (n = 3) after post-hoc analysis across the five treatment groups (asterisk in Fig. 1B; $p < 0.05$).

Figure 1C shows that THP applied to a chain of ganglia also induced periodic bursting in DE-3 (4 preparations). As with DA applied to chains lacking the cephalic ganglion, normal intersegmental phase delays were absent (Puhl and Mesce, 2010).

Fictive crawling and swimming: Pathways and actions of adenylyl cyclase and cAMP

To determine the degree of cAMP elevation caused by IBMX specifically and at the concentration we used to induce bursting, we relied on an enzyme-linked immunosorbant assay (ELISA). Based on an ELISA whereby isolated nerve cords (n = 3) were incubated for 30 min with IBMX, we observed a 128% increase in cAMP (from 12.9 ± 4.9 pmol/ml extract to 29.4 ± 0.96 pmol/ml extract). This measure demonstrated directly that cAMP levels were indeed amplified.

Because DA and PDIs produced similar bursting rhythms, we suspected that they may induce rhythmicity by a similar mechanism or pathway. If, on the other hand, DA and PDIs act through distinct and incompatible pathways, co-application of DA and a PDI should disrupt or degrade rhythmicity. Thus we measured 80 bursts from five IBMX-treated ganglia and 57 bursts from four ganglia treated with both DA and IBMX. For statistical comparisons, mean cycle periods from each ganglion were compared because of the unequal numbers of bursts measured per ganglion. We found that IBMX treatment caused an average cycle period of 20.8 ± 3.1 s (n = 5), while IBMX+DA treatment caused an average cycle period of 21.9 ± 8.7 s (n = 4); a Student's *t*-test yielded no statistically significant difference between these two treatment groups ($t_7 = -0.13$; $p = 0.9$). Whether DA and IBMX converge on a common pathway to induce rhythmicity or act through distinct mechanisms that can be co-activated without interfering with one another must await further study.

It is noteworthy that although the DP nerve recording shown in Fig. 1A showed no units firing (showing that THP can induce bursting in quiescent preparations), other preparations exhibited a mean (pre-treatment) DE-3 tonic discharge rate of 5.4 ± 1.4 Hz

(n = 7; rates averaged over 10-min intervals). Such spontaneous activity is common and has been described elsewhere (Garcia-Perez et al., 2007). We can not yet account for why a few of our isolated ganglia showed very low levels of spontaneous DP nerve activity while others did not.

Because PDIs can activate DE-3 bursting, we reasoned that adenylyl cyclase inhibition might suppress spontaneous neural activity in the DP nerve. To test this idea, we used MDL-12330a, a known inhibitor of adenylyl cyclase that significantly lowers basal cAMP concentrations in leech nervous tissues (Hunt and Evans, 1980; Biondi et al., 1990). We observed that after a 10-30 min application of 0.1-0.5 mM MDL-12330a, only a few DE-3 spikes per min were observed in isolated ganglia. Furthermore, no bursting was ever observed in either DE-3 or in any other units within the DP nerve from isolated ganglia (n = 4) or chains of ganglia (M2 through M19) (n = 3).

THP and other PKA activators, such as DB-cAMP, have previously been shown to be capable of activating fictive swimming (Hashemzadeh-Gargari and Friesen, 1989). In this earlier study, however, fictive crawling had not yet been characterized; thus it was not discussed. Fictive swimming is defined as at least three consecutive DE-3 bursts (typically recorded from the DP nerve) with a cycle period of 0.5-2.0 sec (Ort et al., 1974). The earlier experiments performed by Hashemzadeh-Gargari and Friesen (1989) used chains of ganglia from M2 to M19. In our hands, only one of seven preparations (M2-M19) exhibited fictive swimming when treated with 4-5 mM THP and only one of eight swam spontaneously in 50-200 μM DB-cAMP; we also observed a few swim episodes in two of four chains comprised of seven ganglia treated with THP (data not shown). No swim episodes were observed from isolated single ganglia treated with THP (n = 17) or IBMX (n = 15), although swim induction in single ganglia is infrequent even in response to potent swim-inducing stimuli (Hocker et al., 2000).

Because elements of the crawl CPG (specifically, the elongation network) are thought to be a component of the swim CPG (Esch et al., 2002; Briggman et al., 2005), it is not surprising that some swimming was observed when the crawl CPG was activated. In contrast, when DA is used to activate the crawl CPG, swimming is never observed because DA is a potent inhibitor of the swim CPG (Crisp and Mesce, 2004). Thus we

suggest that THP mimics DA in activating the crawl CPG, but not in suppressing the swim CPG.

Insights into mechanisms underlying PDI-induced bursting

As we showed in Figure 1, THP dissolved in normal leech saline (containing 1.8 mM Ca^{2+}) produced crawl-like DE-3 bursting. Similar bursting, however, has previously been observed in Ca^{2+}-free saline (Angstadt and Friesen, 1991). To determine whether THP-induced bursting requires Ca^{2+} influx, we dissolved THP in saline in which we replaced the Ca^{2+} with equimolar nickel (n = 3) or equimolar cobalt (n = 2). We observed that THP-induced DE-3 bursting in the absence of Ca^{2+} was not statistically different from THP-bursting in the presence of Ca^{2+} with respect to cycle period (t_6 = -0.41, $p > 0.05$) or burst duration (t_6 = -0.86, $p > 0.05$). For example, THP-induced bursting had a cycle period of 20.4 ± 2.4 s (n = 5) in 1.8 mM Ca^{2+} compared to 22.3 ± 4.2 s (n = 3) in 1.8 mM Ni^{2+}. Burst durations appeared to be slightly longer in 1.8 mM Ni^{2+} (7.4 ± 2.7 s) than in 1.8 mM Ca^{2+} (5.5 ± 0.8 s), but this difference was not statistically significant (t_6 = -0.86, $p > 0.05$). THP-induced bursts were not observed when 2 mM $MgCl_2$ (in addition to 1.8 mM Ca^{2+}) was included in the saline (n = 6) or when Ca^{2+} was elevated to 8 mM (n = 5). It is unclear whether these actions are due to interference with Ca^{2+}-dependent mechanisms or a general effect of divalent cations on cellular excitability (Frankenhaeuser and Hodgkin, 1957).

Clotrimazole (CLO), briefly mentioned earlier, is a selective blocker of intermediate conductance Ca^{2+}-dependent K^+ (IK) channels (Engbers et al., 2012; Ishii et al., 1997; Joiner et al., 1997), which are known to be inhibited when phosphorylated by PKA (Neylon et al., 2004). We observed that 25 μM CLO produced bursting in the DP nerve with a cycle period (20.0 ± 2.2 s) similar to DA, THP and IBMX (n = 3) (Fig. 1B). This cycle period was also similar to that previously reported using Ca^{2+} channel blockers (23.2 ± 2.7 s) (Angstadt and Friesen, 1991). However, the mean burst durations observed in CLO were significantly longer (13.5 ± 1.7 s; $p < 0.05$) than bursts observed in DA (5.4 ± 0.6 s), THP (5.5 ± 0.8 s) or IBMX (5.1 ± 0.5 s; Fig. 1B), and longer than previously reported for Ca^{2+} channel blockers (6.6 ± 0.52 s) (Angstadt and Friesen, 1991). Thus, the duty cycle observed in CLO (66%) was considerably longer than that in DA (35%) (Puhl

and Mesce, 2008), THP (37%) or IBMX (28%). CLO has also been reported to inhibit Na^+-K^+ pump activity (Bartolommei et al., 2008); treatments that inhibit this pump, such as oubain (Angstadt and Friesen, 1991) and low extracellular K^+ (Angstadt et al., 1998), have been shown to increase the duration of bursts induced by Ca^{2+} channel blockers in leech neurons.

In saline lacking Ca^{2+} ions, many leech neurons show bursting activity that is dependent on sodium influx (Angstadt and Choo, 1996). To test the hypothesis that PDIs activate bursting that is driven by sodium influx, a series of experiments were conducted in which THP or IBMX were co-applied with riluzole, a sodium channel blocker. Riluzole is known to selectively block the persistent, non-inactivating component of the sodium current while sparing the transient component that is required for normal action potential generation (Kononenko et al., 2004; Niespodziany et al., 2004; Urbani and Belluzzi, 2000). In the leech, riluzole has been shown to impair sodium-dependent PIR but does not interfere with spike generation in motoneurons (Angstadt et al., 2011). We found that 200 μM riluzole was sufficient to block bursting produced by either 4.4 mM THP (n = 3) or 0.5 mM IBMX (n = 4). For example, Figure 2A shows an experiment in which DE-3, in a single ganglion, was induced to burst with IBMX (15 min application). Perfusion of saline containing 200 μM riluzole (with 0.5 mM IBMX) for several minutes halted bursting, although these preparations were still able to fire impulses (Fig. 2B). Removing riluzole, by extensively perfusing the ganglion with saline containing 0.5 mM IBMX only, restored bursting (Fig. 2C). Similarly, a 50% reduction of extracellular sodium ion concentration by substitution with equimolar N-methyl-D-glucamine suppressed THP-induced bursting (n = 3; data not shown). In contrast, 25 μM nifedipine, a blocker of voltage-gated Ca^{2+} channels, did not noticeably affect THP-induced bursting (n = 2; data not shown). Together, these data are consistent with the hypothesis that PDIs activate a bursting mechanism in which sodium influx, rather than Ca^{2+}, drives burst generation.

Phosphodiesterase inhibitors and DA exert distinct effects on specific crawl-related motoneurons

In response to DA, motoneurons DI-1, VI-2 and CV rhythmically burst during the elongation phase of crawling, whereas motoneurons DE-3, VE-4 and AE fire out-of-phase during the contraction phase (Puhl and Mesce, 2008). To determine if DA acts through cAMP-mediated cascades, to promote crawl-like bursting across a wide variety of crawl-related motoneurons, we examined the cells just mentioned in the presence of THP or IBMX. Furthermore, we asked whether the PDIs could substitute, in part, for the network-organizing actions of DA. Because only DE-3 can be effectively monitored via spikes in the DP nerve, intracellular recordings were made from the other motoneurons. In IBMX or THP (0.5 mM and 4.4 mM, respectively), motoneurons DI-1, VI-2, VE-4 and AE not only fired in bursts but they fired during their correct phases. Cell CV was observed to burst; however, it fired incorrectly and was in phase with DE-3 (n = 4; Fig. 3). Because the somata (i.e., recording site) of these motoneurons are electrically inexcitable, their recorded impulses appear small in amplitude. DI-1 and VI-2 are inhibitory motoneurons that become inhibited when the excitatory motoneurons DE-3 and VE-4 are excited during the contraction phase. It is noteworthy that other identified neurons known not to burst during DA-induced or spontaneous crawling were not observed to burst in IBMX or THP; these included the serotonergic Rz cell (n = 8), the touch (T) mechanoreceptor cell (n = 4) and the nociceptive N cell (n = 4). Each of these neurons, in contrast, fires bursts of impulses spontaneously in Ca^{2+}-free saline (Angstadt and Friesen, 1991), indicating that the PDIs are more selective in their actions.

To identify the range of ionic currents modulated by DA via cAMP-dependent mechanisms, we needed first to characterize how the membrane properties of the crawl-related neurons change in the context of DA modulation. To address this issue, we exposed ganglia to a 30-min bath application of 75 μM DA, which is known to induce fictive crawling (Puhl and Mesce, 2008). We used a discontinuous current clamp (DCC) and monitored membrane potential trajectories for 3 s following the termination of a 1-s single depolarizing and single hyperpolarizing current pulse. All neurons were held at -40 mV with current injection during the DCC experiments. Neurons requiring more than ± 0.25 nA to maintain a membrane potential of -40 mV were considered damaged and data from such cells were not analyzed.

For CV, we found an increase in its AHP (area below baseline during 500 ms beginning 50 ms after the end of current injection) that was statistically significant ($F_{1,17}$ = 6.15; $p < 0.05$; n = 9 control, n = 10 in DA). DA increased the mean area below baseline during the AHP from -577 ± 123 mV x ms in NS (n = 9) to -1862 ± 284 mV x ms in DA (n = 10). We also observed a decrease in the duration of its PIR (Fig. 4A, C), which was not associated with a statistically-significant reduction of the area under the curve. The area under the curve of the PIR is a measure of peak membrane potential and duration of sustained change during 500 ms beginning 50 ms after the end of current injection. CV showed a nonsignificant decrease in the mean area under the curve from 3199 ± 530 mV x mS in NS (n = 11) to 2519 ± 517 mV x ms in DA (n = 11). Likely, the similar area measurement was due to a more pronounced peak and shorter time course in DA as compared to the more long-lasting PIR observed in NS. The enhanced peak was associated with a statistically significant increase in firing rate during the PIR in CV, from 8.3 ± 1.1 spikes to 17.2 ± 3.3 spikes in an interval of 500 ms following termination of a 1-s current pulse of -2 nA (t_5 = -2.61, $p < 0.05$).

DA significantly decreased the duration of the PIR in AE ($F_{1,7}$ = 8.96; $p < 0.05$; n = 5 control, n = 4 in DA). The mean area under the curve decreased from 1624 ± 328 mV x ms in NS (n = 10) to 499 ± 61 mV x ms in DA (n = 10). The effect on its AHP was less pronounced (Fig. 4B, D) and not statistically significant. The area under baseline during the AHP decreased from 1067 ± 81 mV x ms in NS (n = 10) to 873 ± 286 mV x ms in DA (n = 10). The PIR in leech motoneurons appears to have an early component and a late component (Angstadt et al., 2011); it is the late component that appears to be diminished following DA treatment in AE. It has been previously reported that DA causes a statistically significant increase in the peak amplitude of the PIR in DE-3, but not the area under the curve (Vallecorsa et al., 2007).

An increase in overall cellular excitability is one way that neuromodulators can exert their influence over CPG activation (Clemens and Katz, 2003; Dai et al., 1998; Fedirchuk and Dai, 2004; Katz, 1998; Katz and Frost, 1997). Based on firing frequency, as an indicator of cell excitability, we found that DA reduced neuronal excitability, but only in the context of current injection. We again used a DCC protocol but one that stepped cells from -2 to +2 nA in steps of +0.5 nA. In normal saline, AE fired impulses

tonically at a rate of 5.8 ± 1.5 Hz (n = 4), close to its resting firing rate when treated with 75 µM DA (6.6 ± 0.7 Hz; n = 5). However, when treated with DA, a +1 nA current pulse increased the spike firing frequency of AE only to 12.6 ± 2.1 Hz (n = 5) as compared to 18 ± 2.3 Hz (n = 4) in normal saline (Fig. 5A). This difference was even greater in CV, where again the resting firing rates were similar in saline and DA [(9.0 ± 1.8 Hz, control (n = 8) vs 6.0 ± 1.6 Hz, in DA (n = 8); (Fig. 5B)]. A +1 nA current injection increased the firing frequency of CV only to 23.0 ± 3.0 Hz in DA as compared to 41.2 ± 3.8 Hz in normal saline. These results are consistent with prior observations that DA exerts a generally inhibitory influence on leech neurons (Ali et al., 1998; Crisp and Mesce, 2004; Sargent, 1975), but helps to enhance their patterned activity.

We next asked whether mimicking DA_1 receptor activation with THP can cause the full range of DA-induced physiological changes in motoneurons just presented. In contrast to the direct effects of DA, bath application of 4.4 mM THP for 20-40 min did not noticeably enhance the PIR of CV (n = 4; data not shown), nor did it mimic the effect of DA on the excitability of CV (n = 4; Fig 5C) or AE (n = 6; Fig 5D). For example, injection of +1 nA positive current resulted in a firing rate of 18.0 ± 2.3 Hz in normal saline and 20.0 ± 2.2 Hz in THP. In addition, while DA only caused a slight increase in the resting discharge rate of the AE cell (from 4.0 ± 1.5 Hz in normal saline to 6.6 ± 0.8 Hz in DA), THP also caused an increase in resting discharge rate (15.2 ± 3.8 Hz). Similarly, the resting discharge rate for CV was 9.0 ± 1.8 Hz in normal saline but 17.8 ± 3.7 Hz in THP (n = 4). On the other hand, THP diminished or eliminated the PIR in the AE cell (n = 6; data not shown). ANOVAs were employed to analyze the effects of DA, THP and NS on the resting discharge rates and slopes of the F-I curves in Fig. 5C, D. There was a significant effect of treatment on cell CV ($F_{4,34} = 5.11$; $p < 0.01$), and Fisher LSD post-hoc tests revealed that DA caused a significant reduction in slope compared to NS ($p < 0.05$); there was no significant difference between the effect of THP and NS on slope. THP caused a significant increase in resting discharge rate compared to DA ($p < 0.05$) and NS ($p < 0.01$). Similarly, there was a significant effect of treatment on AE ($F_{4,22} = 8.13$; $p < 0.001$) and post-hoc tests revealed that DA caused significant reduction in slope compared to NS ($p < 0.05$). THP was not different from either DA or NS with respect to slope, but was significantly different from DA ($p < 0.001$) and NS ($p < 0.001$)

with respect to resting discharge rate. These results indicate that DA is likely affecting crawl-related targets by modulating a number of DA receptor-mediated pathways beyond a DA_1-like type.

DISCUSSION

Here we have demonstrated several cellular mechanisms that may be involved in the DA induction of fictive crawl-related bursting in leech ganglia. Specifically, we have shown that elevating cAMP by inhibiting PDE activity induces robust DE-3 motoneuron bursting that resembles DA-activated fictive crawling. This bursting activity relies on a sodium rather than a Ca^{2+} influx. Furthermore, bursting with a similar cycle period can be induced by pharmacologically inhibiting a Ca^{2+}-dependent K^+ current, specifically, an IK-like current. We have also shown, through intracellular recordings, that DA modulates the intrinsic membrane properties of a variety of crawl-related motoneurons in ways that may facilitate participation in patterned bursting. Not all the actions of DA, however, can be mimicked by inhibiting PDE activities, suggesting the involvement of non DA_1-like receptors not positively-coupled to cAMP.

We suggest that DA activates crawling through at least two pathways, only one of which is mimicked by THP. In one pathway, an extrinsic oscillator or timing network is activated that is capable of generating crawl-like bursting in leech motoneurons. This timing mechanism, under experimental conditions, is capable of driving the crawl or swim CPG, but in the presence of DA will induce only crawling as DA is known to be a potent inhibitor of swimming (Crisp and Mesce, 2004). This timing mechanism may be a separate module of the CPG from that responsible for generating the phase relationships among the motoneurons. Occasionally, in recordings of fictive walking and scratching in cats, some motoneuron pools fail to fire during their appropriate phase in the rhythm, but the cycle period remains unaffected by this deletion, suggesting a dissociation of the timing mechanism from the motoneuron patterning network (Lafreniere-Roula and McCrea, 2005; Rybak et al., 2006). These observations suggest that some CPGs may possess independent timing elements that govern the overall temporal structure of the motor pattern (e.g., cycle period) and patterning elements that govern motor neuron activity within the cycle (e.g., phase relationships).

The second action of DA, which is not readily mimicked by THP, consists of the modification of excitability and afterpotentials of motoneurons. While this latter function may be related to a general inhibitory function of DA that helps to suppress incompatible motor behaviors (i.e., swimming), modulation of dynamic membrane properties may help motoneurons to maintain firing patterns that follow a rhythmic excitatory drive with fidelity.

Induction of Bursting in Leech Neurons

Leech neurons that are normally quiescent at rest can be induced to burst through several pharmacological manipulations. For example, in all leech neurons examined to date, a persistent sodium current will drive sodium plateau potentials resulting in rhythmic bursting unless this inward current is opposed by Ca^{2+}-dependent K^+ currents. This rhythmic bursting activity is evident when leech neurons are treated with Ca^{2+} channel blockers (Angstadt and Friesen, 1991). Ca^{2+}-dependent K^+ and persistent sodium currents have opposing effects on excitability (Burrell and Crisp, 2008; Wu et al., 2005) and contribute to oscillations and bursting in various ways across different neuronal types (Boehmer et al., 2000; Gutfreund et al., 1995; Hu et al., 2002). Our finding that riluzole (a blocker of the persistent sodium current) impairs PDI-induced bursting, in contrast to Ca^{2+}channel blockers such as cobalt, supports the hypothesis that DA acts through a cAMP-dependent pathway to activate a bursting mechanism involving sodium-based plateau potentials. A persistent sodium channel has been found to be a target of PKA in *Lymnaea* (Nikitin et al., 2006), suggesting a potential biochemical connection between cAMP concentrations and sodium plateau generation.

While enhancing persistent sodium currents or blocking Ca^{2+}-dependent K^+ currents seem like plausible means by which PDIs may activate elements of the crawl oscillator, the effects of DA on CV and AE would be better explained by opposite effects on these currents. Recently, blocking persistent sodium currents with riluzole has been shown to *reduce* the late component of the PIR and block bursting in cell DE-3 (Angstadt et al., 2011), unlike DA, which attenuates the PIR and *promotes* bursting. Furthermore, while reduced sodium salines decrease PIR in DE-3, the PIR is eliminated only when sodium is reduced and Ca^{2+} is replaced with nickel (Angstadt et al., 2005) or in solutions

containing high concentrations (10 mM) of nickel (Angstadt et al., 2011). These observations suggest that a portion of the PIR is Ca^{2+}-dependent and suggest that the PIR is mediated by both persistent sodium and nonspecific cation currents.

If DA activates oscillations by unmasking or potentiating a persistent sodium current, one might also expect an increase in excitability and PIR in cells modulated by this mechanism. However, even if DA enhances the persistent sodium current in specific motoneurons, the ability of such a change to increase excitability may be limited by the cell's input resistance, the extent of its electrical coupling and the expression of other currents contributing to the whole cell I-V curve (Zhao et al., 2010). Furthermore, DA may diminish PIR in DE-3 cells through combined mechanisms, such as enhancing a Ca^{2+}-dependent K^+ conductance, inhibiting the riluzole-sensitive persistent sodium current or inhibiting a Ca^{2+}-dependent nonspecific cation current (Angstadt et al., 2011). Any of these mechanisms could contribute to a decrease in excitability.

Implication of Multiple DA Receptor Subtypes

The opposing actions of DA_1 and DA_2 receptors were characterized in the mollusc *Lymnaea* almost 30 years ago (Stoof et al., 1984), and newer cell-molecular and pharmacological studies have suggested the presence of at least three classes of DA receptors in invertebrates (Mustard et al., 2005). In the lobster stomatogastric nervous system, DA has been shown to be an important modulator altering motor pattern expression (Ayali and Harris-Warrick, 1999; Mullins et al., 2011; Vidal-Gadea et al., 2011). DA's action are often mediated through multiple and sometimes opposing modulatory effects on neurons within a given circuit. For example, DA enhances an A-type K^+ conductance in the pyloric dilator neuron (Kloppenburg et al., 1999), but depresses this same conductance in the lateral pyloric neuron (Harris-Warrick et al., 1995). These opposing actions can be explained by the expression of DA_1 (but not DA_2) receptors in the lateral pyloric neuron and DA_2 (but not DA_1) receptors in the pyloric dilator neuron (Zhang et al., 2010).

Although previous evidence suggests the presence of a DA_1-like receptor in the leech (Ali et al., 1998; Colombaioni and Brunelli, 1988; Salzet et al., 1998), the pharmacological properties of this receptor and other sub-types may be distinct from

other species. The leech likely has a second class of DA receptors not positively coupled to cAMP. For example, DA but not cAMP inhibit ion transport across leech skin (Milde et al., 2001). Similarly, not all the effects of DA on the crawl circuit can be mimicked by PDIs, as evidenced by the improper phase relationships of DE-3 and CV and the inability of THP to reduce motoneuron excitability. Preliminary studies show that apomorphine, a possible DA_2–like agonist in leech, can induce crawl-like bursting with CV in phase with DE-3 (Puhl and Mesce, personal communication). The DA_2-receptor family contains receptors that are negatively coupled to adenylyl cyclase, and while no DA_2-like receptor has yet to be characterized pharmacologically in *Hirudo,* genes for several DA_2-receptor families have been identified in the leech *Helobdella robusta* (EMBL-EBI accession numbers IPR 001620, IPR 001922 & IPR 002185).

Behavioral Significance of DA Modulation of Motoneurons

Modulation of crawl motoneurons may reflect two parallel actions of DA. First, DA modulates membrane properties known to contribute to rhythm generation. After DA treatment, CV shows an enhanced AHP and a higher firing frequency during the peak PIR. Interestingly, no statistically significant increase in AHP was observed in either DE-3 or AE, although DE-3 showed an enhanced peak in its PIR (Vallecorsa et al., 2007). DE-3 and CV innervate the longitudinal and circular muscles, respectively, and both of these are body wall muscles that are directly responsible for locomotor movements. In contrast, AE innervates the annular erector musculature, and the role of annular erection in crawling is less clear, though it may aid in traction. Possibly for this reason, AE bursts late in contraction (Eisenhart et al., 2000), giving it a somewhat unique phase relationship to the other motoneurons that may be reflected in its unique pattern of modulatory changes.

It is not yet clear how a DA-induced decrease in motoneuron excitability would facilitate the expression of rhythmic bursting during fictive crawling. Quite to the contrary, it seems that an increase in excitability would be more likely to promote bursting in leech motoneurons. A decreased excitability may, however, contribute to a generalized inhibitory effect of DA that could help to suppress the expression of incompatible behaviors, especially swimming (Crisp and Mesce, 2004). Furthermore, the

duration and firing frequencies exhibited by locomotor motoneurons affect both the rate of muscle contraction and time to peak contraction. Thus, a decrease in excitability may well facilitate the ability of each body segment to transition smoothly from any given body length, enabling the metachronal waves of crawl activity to progress gracefully along the animal's body as it repeatedly elongates and shortens. One overarching lesson gleaned from our studies is that DA has the ability to activate a mosaic of cellular actions. Answers to how each of these pieces complement the other to form a coherent locomotor behavior will certainly benefit from future characterizations of leech-specific DA receptor sub-types.

ACKNOWLEDGEMENTS

We thank Drs. William B. Kristan, Jr. and James Angstadt for helpful discussions and insights throughout our study and thank Dr. Josh Puhl, Ms. Windy Lynch, Mr. Bilal Alkatout and Ms. Nicole Marvin for technical assistance. We are also most grateful to the expert anonymous reviewers whose helpful suggestions greatly strengthened the final version of our manuscript.

FUNDING

This research was supported by NSF grants (IOS-0924119) awarded to K.M.C. and (IOS-0924155) to K.A.M.

FIGURE LEGENDS

Figure 1. The phosphodiesterase inhibitor (PDI) theophylline (THP) caused bursting activity in motoneuron DE-3 (largest unit) recorded from the dorsal posterior (DP) nerve. (A) Activity in the DP nerve of a single, isolated ganglion was quiescent in normal saline (NS) after 20 min (top trace), but became rhythmically active after a 10-20 min exposure to 4.4 mM THP (middle trace) (13 of 15 preparations). Bursting was not induced by exposing ganglia for up to 30 min in the adenosine receptor blocker 8(p-sulfophenyl) theophylline (SPL; 4.4 mM) (bottom trace, different preparation, n = 3). (B) Statistical analyses of burst periods and durations induced by 75 μM DA, 4.4 mM THP, 0.5 mM IBMX and 25 μM clotrimazole (CLO; an IK channel blocker) was compared across all

treatment groups (n = 10 for each group, except n = 3 for CLO). Drugs were applied to single, isolated ganglia. Bursting in these groups was also compared with crawl bursts collected during spontaneous fictive crawling exhibited in isolated whole nerve cords (labeled CNS in NS without DA) (n = 10). DA and CNS raw data were obtained from DA studies originally reported in Puhl and Mesce (2008) and reanalyzed here for comparison. Asterisk represents the only statistically significant difference between treatment conditions: burst durations in CLO were longer than in other conditions ($p < 0.01$). Error bars represent the standard error of the mean. (C) THP-induced bursting in DP nerves (4.4 mM) across chains of ganglia (n = 4). Note that normal intersegmental delays, however, are lacking due to absence of the cephalic ganglion, shown previously to be necessary for intersegmental coordination of the crawl oscillators (Puhl and Mesce, 2010).

Figure 2. IBMX-induced crawl-like bursting in DE-3 is reversibly inhibited by 200 μM riluzole (n = 4), a sodium channel blocker that impairs the persistent sodium current while sparing the transient component (Angstadt et al., 2011; Kononenko et al., 2004; Niespodziany et al., 2004; Urbani and Belluzzi, 2000). (A) 0.5 mM IBMX induced crawl-like DE-3 bursting in the DP nerve of a single, isolated ganglion. (B) Perfusion of 0.5 mM IBMX + 200 μM riluzole, at a rate of 1-2 ml/min, inhibited this bursting in the same ganglion as in (A). (C) Washout with 0.5 mM IBMX (without riluzole) restored bursting.

Figure 3. IBMX-induced crawl-like bursting and crawl-network activation across identified crawl motoneurons. Intracellular recordings from various motoneurons were made while recording DE-3 extracellular activity in the DP nerve. (A, C) Similar to DA-induced fictive crawling, the inhibitory motoneurons DI-1 (A) and VI-2 (C) were hyperpolarized during DE-3 bursting. (B) The excitatory VE-4 motoneuron was depolarized during DE-3 activity, as it normally is during DA application. (D) Unlike fictive crawling, IBMX caused CV bursting that appeared in phase with DE-3 (recorded via DP nerve). Note: Intracellular spike amplitudes are typically small and often overlay

larger synaptic potentials because spike-generating zones are distal to the recording sites (i.e., somata), which are relatively inexcitable in the leech.

Figure 4. Dopaminergic modulation of the dynamic membrane properties of crawl-related motoneurons CV and AE. (A) DA (75 μM) increased the peak amplitude, but attenuated the duration of the post-inhibitory rebound (PIR) in CV; the afterhyperpolarization (AHP) was enhanced. (B) DA shortened the PIR duration in AE and enhanced the duration of the AHP. Dotted lines in (A) and (B) indicate the resting membrane potential as determined prior to stimulation. (C) Summary of area-under-the-curve measurements of PIR and AHP in CV in normal saline (NS) (n = 14) and in DA (n = 11). (D) Summary of area-under-the-curve measurements of PIR and AHP in AE in NS (n = 7) and in DA (n = 10). Asterisks indicate statistically significant differences ($p < 0.05$).

Figure 5. Dopaminergic modulation of excitability of the crawl motoneurons CV and AE. (A) A 1-sec pulse of +1 nA depolarizing elicits a 24 Hz response from AE in NS, but only an 18 Hz response in DA. (B) Injection of a 1-sec pulse of +1 nA depolarizing current elicits a 30 Hz response from CV in NS, but only 25 Hz in 75 μM DA. (C) F-I curves of AE in NS (n = 4), DA (n = 5) and THP (n = 6). (D) F-I curves depicting steady state firing as a function of input current of CV in NS (n = 9), DA (n = 8) and the PDI theophylline (THP; n = 4). In both graphs (C) and (D), the resting discharge rate (0 nA injected current) in THP was statistically different relative to NS or DA ($p < 0.05$), and the slope of the F-I curve in DA was statistically different relative to NS or THP ($p < 0.05$); see Results for details of the statistical analysis.

REFERENCES

Ali, D. W., Catarsi, S. and Drapeau, P. (1998). Ionotropic and metabotropic activation of a neuronal chloride channel by serotonin and dopamine in the leech *Hirudo medicinalis*. *J Physiol* **509**, 211-9.

Angstadt, J. D. and Choo, J. J. (1996) Sodium-dependent plateau potentials in cultured Retzius cells of the medicinal leech. *J Neurophysiol* **76**, 1491-1502.

Angstadt, J. D., Choo, J. J. and Saran, A. M. (1998). Effects of transition metal ions on spontaneous electrical activity and chemical synaptic transmission of neurons in the medicinal leech. *J Comp Physiol A* **182**, 389-401.

Angstadt, J. D. and Friesen, W. O. (1991). Synchronized oscillatory activity in leech neurons induced by calcium channel blockers. *J Neurophysiol* **66**, 1858-73.

Angstadt, J. D., Grassmann, J. L., Theriault, K. M. and Levasseur, S. M. (2005). Mechanisms of postinhibitory rebound and its modulation by serotonin in excitatory swim motor neurons of the medicinal leech. *J Comp Physiol A* **191**, 715-32.

Angstadt, J. D., Simone, A. M. and Peters, N. V. (2011). Effects of riluzole on cell DE-3 of the medicinal leech: Evidence that a persistent sodium current contributes to postinhibitory rebound responses and bursting activity induced by calcium-channel blockers. *2011 Neuroscience Meeting Planner* **Program No. 918.01**, Washington, DC: Society for Neuroscience. Online.

Ayali, A. and Harris-Warrick, R. M. (1999). Monoamine control of the pacemaker kernel and cycle frequency in the lobster pyloric network. *J Neurosci* **19**, 6712-22.

Bartolommei, G., Devaux, N., Tadini-Buoninsegni, F., Moncelli, M. and Apell, H. J. (2008). Effect of clotrimazole on the pump cycle of the Na,K-ATPase. *Biophys J* **95**, 1813-25.

Biondi, C., Campi, A. L., Pareschi, M. C., Portolan, A. and Ferretti, M. E. (1990). RMI 12330A, an inhibitor of adenylate cyclase and cyclic AMP-phosphodiesterase activities in the segmental ganglia of the leech *Hirudo medicinalis.* *Neurosci Lett* **113**, 322-7.

Boehmer, G., Greffrath, W., Martin, E. and Hermann, S. (2000). Subthreshold oscillation of the membrane potential in magnocellular neurones of the rat supraoptic nucleus. *J Physiol* **526**, 115-28.

Briggman, K. L., Abarbanel, H. D. and Kristan, W. B., Jr. (2005). Optical imaging of neuronal populations during decision-making. *Science* **307**, 896-901.

Burrell, B. D. and Crisp, K. M. (2008). Serotonergic modulation of afterhyperpolarization in a neuron that contributes to learning in the leech. *J Neurophysiol* **99**, 605-16.

Burrell, B. D. and Sahley, C. L. (2001). Learning in simple systems. *Curr Opin Neurobiol* **11**, 757-64.

Chandler, S. H. and Goldberg, L. J. (1984). Differentiation of the neural pathways mediating cortically induced and dopaminergic activation of the central pattern generator (CPG) for rhythmical jaw movements in the anesthetized guinea pig. *Brain Res* **323**, 297-301.

Clemens, S., Calin-Jageman, R., Sakurai, A. and Katz, P. S. (2007). Altering cAMP levels within a central pattern generator modifies or disrupts rhythmic motor output. *J Comp Physiol A* **193**, 1265-71.

Clemens, S. and Katz, P. S. (2003). G protein signaling in a neuronal network is necessary for rhythmic motor pattern production. *J Neurophysiol* **89**, 762-72.

Colombaioni, L. and Brunelli, M. (1988). Neurotransmitter-induced modulation of an electrotonic synapse in the CNS of *Hirudo medicinalis*. *Exp Biol* **47**, 139-44.

Crisp, K. M. and Mesce, K. A. (2004). A cephalic projection neuron involved in locomotion is dye coupled to the dopaminergic neural network in the medicinal leech. *J Exp Biol* **207**, 4535-42.

Crisp, K. M. and Muller, K. J. (2006). A 3-synapse positive feedback loop regulates the excitability of an interneuron critical for sensitization in the leech. *J Neurosci* **26**, 3524-31.

Dai, Y., Jones, K. E., Fedirchuk, B., Krawitz, S. and Jordan, L. M. (1998). Modeling the lowering of motoneuron voltage threshold during fictive locomotion. *Ann N Y Acad Sci* **860**, 492-5.

Eisenhart, F. J., Cacciatore, T. W. and Kristan, W. B., Jr. (2000). A central pattern generator underlies crawling in the medicinal leech. *J Comp Physiol A* **186**, 631-43.

Engbers, J. D., Anderson, D., Asmara, H., Rehak, R., Mehaffey, W. H., Hameed, S., McKay, B. E., Kruskic, M., Zamponi, G. W. and Turner, R. W. (2012). Intermediate conductance calcium-activated potassium channels modulate summation of parallel fiber input in cerebellar Purkinje cells. *Proc Natl Acad Sci U S A* **109**, 2601-6.

Esch, T., Mesce, K. A. and Kristan, W. B. (2002). Evidence for sequential decision making in the medicinal leech. *J Neurosci* **22**, 11045-54.

Fedirchuk, B. and Dai, Y. (2004). Monoamines increase the excitability of spinal neurones in the neonatal rat by hyperpolarizing the threshold for action potential production. *J Physiol* **557**, 355-61.

Flamm, R. E. and Harris-Warrick, R. M. (1986). Aminergic modulation in lobster stomatogastric ganglion. I. Effects on motor pattern and activity of neurons within the pyloric circuit. *J Neurophysiol* **55**, 847-65.

Frankenhaeuser, B. and Hodgkin, A. L. (1957). The action of calcium on the electrical properties of squid axons. *J Physiol* **137**, 218-44.

Garcia-Perez, E., Mazzoni, A. and Torre, V. (2007). Spontaneous electrical activity and behavior in the leech *Hirudo medicinalis*. *Front Integr Neurosci* **1**, 8.

Gutfreund, Y., Yarom, Y. and Segev, I. (1995). Subthreshold oscillations and resonant frequency in guinea-pig cortical neurons: physiology and modelling. *J Physiol* **483**, 621-40.

Harris-Warrick, R. M., Coniglio, L. M., Levini, R. M., Gueron, S. and Guckenheimer, J. (1995). Dopamine modulation of two subthreshold currents produces phase shifts in activity of an identified motoneuron. *J Neurophysiol* **74**, 1404-20.

Hashemzadeh-Gargari, H. and Friesen, W. O. (1989). Modulation of swimming activity in the medicinal leech by serotonin and octopamine. *Comp Biochem Physiol C* **94**, 295-302.

Hocker, C. G., Yu, X. and Friesen, W. O. (2000). Functionally heterogeneous segmental oscillators generate swimming in the medical leech. *J Comp Physiol A* **186**, 871-83.

Hu, H., Vervaeke, K. and Storm, J. F. (2002). Two forms of electrical resonance at theta frequencies, generated by M-current, h-current and persistent Na^+ current in rat hippocampal pyramidal cells. *J Physiol* **545**, 783-805.

Hunt, N. H. and Evans, T. (1980). RMI 12330A, an inhibitor of cyclic nucleotide phosphodiesterases and adenylate cyclase in kidney preparations. *Biochim Biophys Acta* **613,** 499-506.

Ishii, T. M., Silvia, C., Hirschberg, B., Bond, C. T., Adelman, J. P. and Maylie, J. (1997). A human intermediate conductance calcium-activated potassium channel. *Proc Natl Acad Sci U S A* **94**, 11651-6.

Joiner, W. J., Wang, L. Y., Tang, M. D. and Kaczmarek, L. K. (1997). hSK4, a member of a novel subfamily of calcium-activated potassium channels. *Proc Natl Acad Sci U S A* **94**, 11013-8.

Katz, P. S. (1998). Neuromodulation intrinsic to the central pattern generator for escape swimming in *Tritonia*. *Ann N Y Acad Sci* **860**, 181-8.

Katz, P. S. and Frost, W. N. (1997). Removal of spike frequency adaptation via neuromodulation intrinsic to the *Tritonia* escape swim central pattern generator. *J Neurosci* **17**, 7703-13.

Kemnitz, C. P. (1997). Dopaminergic modulation of spinal neurons and synaptic potentials in the lamprey spinal cord. *J Neurophysiol* **77**, 289-98.

Kloppenburg, P., Levini, R. M. and Harris-Warrick, R. M. (1999). Dopamine modulates two potassium currents and inhibits the intrinsic firing properties of an identified motor neuron in a central pattern generator network. *J Neurophysiol* **81**, 29-38.

Kononenko, N. I., Shao, L. R. and Dudek, F. E. (2004). Riluzole-sensitive slowly inactivating sodium current in rat suprachiasmatic nucleus neurons. *J Neurophysiol* **91**, 710-8.

Kristan, W. B., Jr., Calabrese, R. L. and Friesen, W. O. (2005). Neuronal control of leech behavior. *Prog Neurobiol* **76**, 279-327.

Lafreniere-Roula, M. and McCrea, D. A. (2005). Deletions of rhythmic motoneuron activity during fictive locomotion and scratch provide clues to the organization of the mammalian central pattern generator. *J Neurophysiol* **94**, 1120-32.

Lapointe, N. P., Rouleau, P., Ung, R. V. and Guertin, P. A. (2009). Specific role of dopamine D1 receptors in spinal network activation and rhythmic movement induction in vertebrates. *J Physiol* **587**, 1499-511.

Mesce, K. A. and Pierce-Shimomura, J. T. (2010). Shared strategies for behavioral switching: understanding how locomotor patterns are turned on and off. *Front Behav Neurosci* **4**, article 49, 1-5.

Milde, H., Weber, W. M., Salzet, M. and Clauss, W. (2001). Regulation of Na^+ transport across leech skin by peptide hormones and neurotransmitters. *J Exp Biol* **204**, 1509-17.

Mink, J. W. (1996). The basal ganglia: focused selection and inhibition of competing motor programs. *Prog Neurobiol* **50**, 381-425.

Mullins, O. J., Hackett, J. T., Buchanan, J. T. and Friesen, W. O. (2011). Neuronal control of swimming behavior: comparison of vertebrate and invertebrate model systems. *Prog Neurobiol* **93**, 244-69.

Mustard, J. A., Beggs, K. T. and Mercer, A. R. (2005). Molecular biology of the invertebrate dopamine receptors. *Arch Insect Biochem Physiol* **59**, 103-17.

Neylon, C. B., D'Souza, T. and Reinhart, P. H. (2004). Protein kinase A inhibits intermediate conductance Ca^{2+}-activated K^+ channels expressed in *Xenopus oocytes*. *Pflugers Arch* **448**, 613-20.

Nicholls, J. G. and Baylor, D. A. (1968). Specific modalities and receptive fields of sensory neurons in CNS of the leech. *J Neurophysiol* **31**, 740-56.

Niespodziany, I., Klitgaard, H. and Margineanu, D. G. (2004). Is the persistent sodium current a specific target of anti-absence drugs? *Neuroreport* **15**, 1049-52.

Nikitin, E. S., Kiss, T., Staras, K., O'Shea, M., Benjamin, P. R. and Kemenes, G. (2006). Persistent sodium current is a target for cAMP-induced neuronal plasticity in a state-setting modulatory interneuron. *J Neurophysiol* **95**, 453-63.

Ort, C. A., Kristan, W. B. and Stent, G. S. (1974). Neuronal control of swimming in the medicinal leech. II. Identification and connections of motor neurons. *J Comp Physiol* **94**, 121-154.

Puhl, J. G. and Mesce, K. A. (2008). Dopamine activates the motor pattern for crawling in the medicinal leech. *J Neurosci* **28**, 4192-200.

Puhl, J. G. and Mesce, K. A. (2010). Keeping it together: mechanisms of intersegmental coordination for a flexible locomotor behavior. *J Neurosci* **30**, 2373-83.

Quinlan, E. M., Arnett, B. C. and Murphy, A. D. (1997). Feeding stimulants activate an identified dopaminergic interneuron that induces the feeding motor program in *Helisoma*. *J Neurophysiol* **78**, 812-24.

Rybak, I. A., Shevtsova, N. A., Lafreniere-Roula, M. and McCrea, D. A. (2006). Modelling spinal circuitry involved in locomotor pattern generation: insights from deletions during fictive locomotion. *J Physiol* **577**, 617-39.

Salzet, B., Stefano, G. B., Verger-Bocquet, M. and Salzet, M. (1998). Putative leech dopamine1D1-like receptor molecular characterization: sequence homologies between dopamine and serotonin leech CNS receptors explain pharmacological cross-reactivities. *Brain Res Mol Brain Res* **58**, 47-58.

Sargent, P. B. (1975). Transmitters in the leech central nervous system: analysis of sensory and motor cells. PhD thesis, Harvard University, Cambridge.

Sawin, E. R., Ranganathan, R. and Horvitz, H. R. (2000). *Caenorhabditis elegans* locomotory rate is modulated by the environment through a dopaminergic pathway and by experience through a serotonergic pathway. *Neuron* **26**, 619-31.

Smith, Y., Bevan, M. D., Shink, E. and Bolam, J. P. (1998). Microcircuitry of the direct and indirect pathways of the basal ganglia. *Neuroscience* **86**, 353-87.

Stoof, J. C., De Vlieger, T. A. and Lodder, J. C. (1984). Opposing roles for D1 and D2 dopamine receptors in regulating the excitability of growth hormone-producing cells in the snail *Lymnaea stagnalis*. *Eur J Pharmacol* **106**, 431-5.

Teyke, T., Rosen, S. C., Weiss, K. R. and Kupfermann, I. (1993). Dopaminergic neuron B20 generates rhythmic neuronal activity in the feeding motor circuitry of *Aplysia*. *Brain Res* **630**, 226-37.

Urbani, A. and Belluzzi, O. (2000). Riluzole inhibits the persistent sodium current in mammalian CNS neurons. *Eur J Neurosci* **12**, 3567-74.

Vallecorsa, G. M., Amatrudo, J. M. and Angstadt, J. D. (2007). Dopamine induces rhythmic activity and enhances postinhibitory rebound in a leech motor neuron involved in swimming and crawling behaviors. *Impulse* **4**, online.

Vidal-Gadea, A., Topper, S., Young, L., Crisp, A., Kressin, L., Elbel, E., Maples, T., Brauner, M., Erbguth, K., Axelrod, A. et al. (2011). *Caenorhabditis elegans* selects distinct crawling and swimming gaits via dopamine and serotonin. *Proc Natl Acad Sci U S A* **108**, 17504-9.

Wu, N., Enomoto, A., Tanaka, S., Hsiao, C. F., Nykamp, D. Q., Izhikevich, E. and Chandler, S. H. (2005). Persistent sodium currents in mesencephalic v neurons participate in burst generation and control of membrane excitability. *J Neurophysiol* **93**, 2710-22.

Zhang, H., Rodgers, E. W., Krenz, W. D., Clark, M. C. and Baro, D. J. (2010). Cell specific dopamine modulation of the transient potassium current in the pyloric network by the canonical D1 receptor signal transduction cascade. *J Neurophysiol* **104**, 873-84.

Zhao, S., Golowasch, J. and Nadim, F. (2010). Pacemaker neuron and network oscillations depend on a neuromodulator-regulated linear current. *Front Behav Neurosci* **4**, article 21, 1-9.

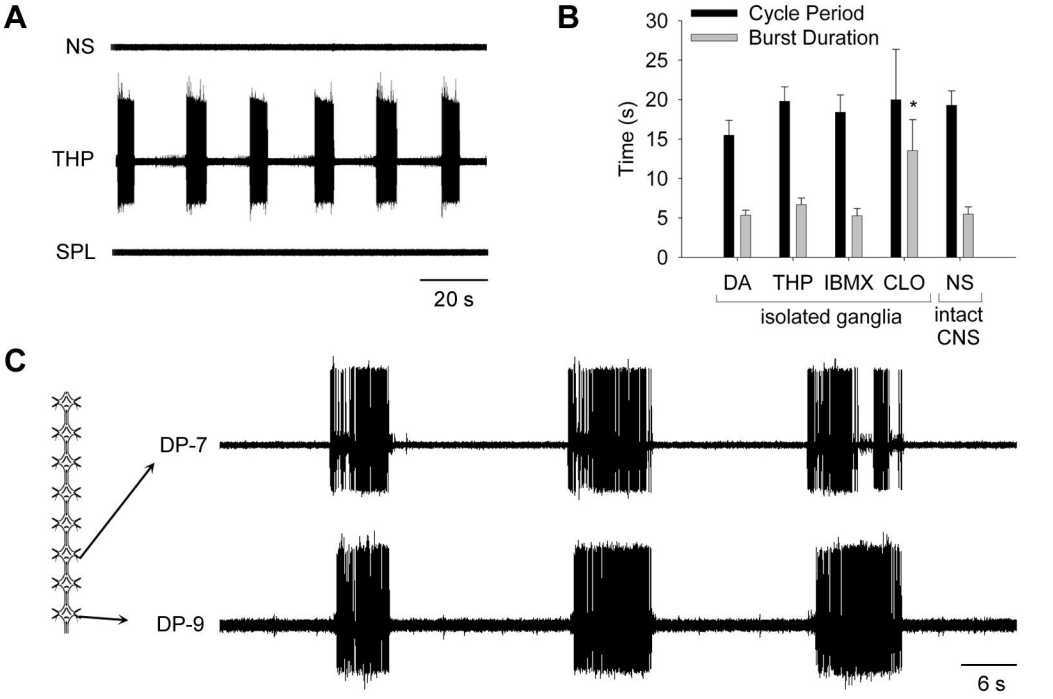
A
NS
THP
SPL
20 s
B
Cycle Period
Burst Duration
Time (s)
30
25
20
15
10
5
0
*
DA
THP
IBMX
CLO
NS
isolated ganglia
intact CNS
C
DP-7
DP-9
6 s

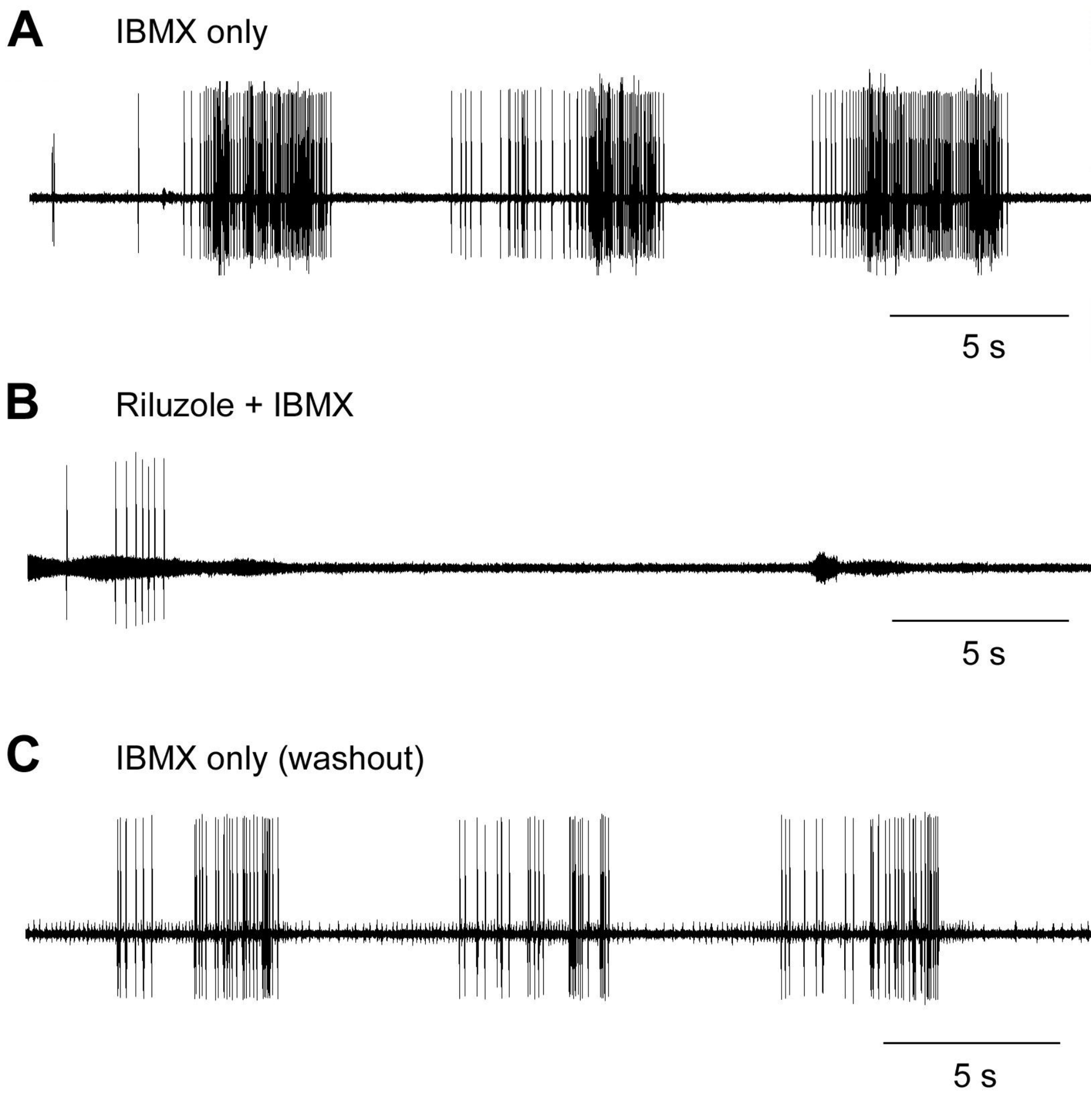
A
IBMX only
5 s
B
Riluzole + IBMX
5 s
C
IBMX only (washout)
5 s

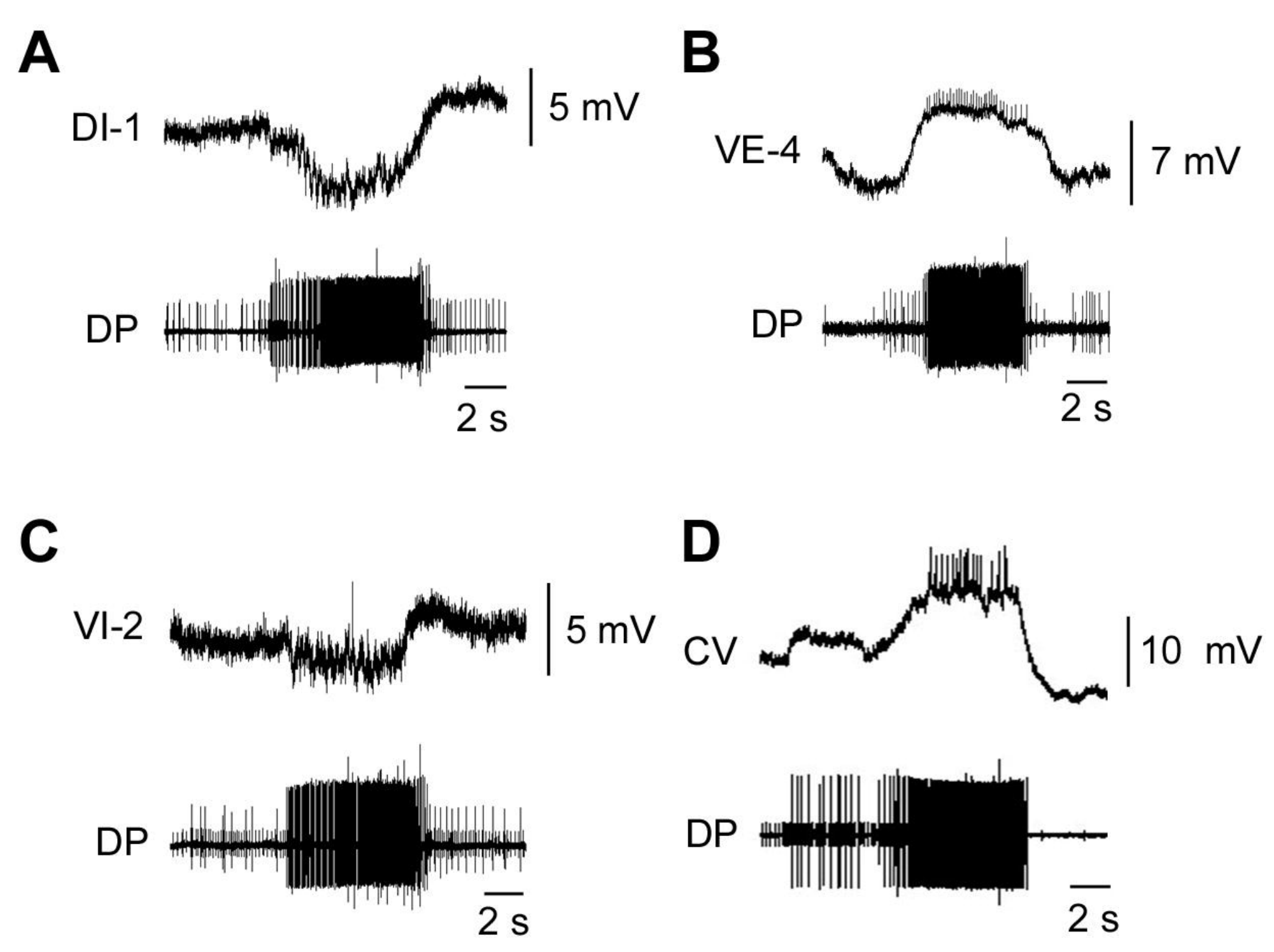
A
DI-1
5 mV
DP
2 s
B
VE-4
7 mV
DP
2 s
C
VI-2
5 mV
DP
2 s
D
CV
10 mV
DP
2 s

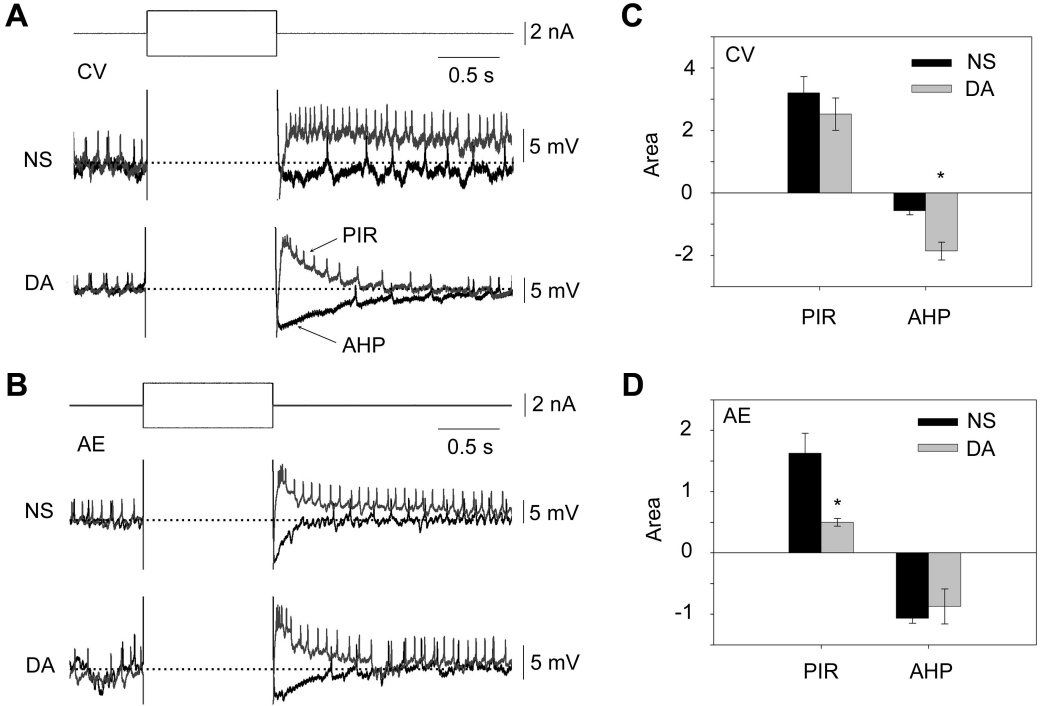
A
2 nA
CV
0.5 s
NS
5 mV
PIR
DA
5 mV
AHP
B
2 nA
AE
0.5 s
NS
5 mV
DA
5 mV
C
CV
NS
DA
Area
4
2
0
-2
*
PIR
AHP
D
AE
NS
DA
Area
2
1
0
-1
*
PIR
AHP

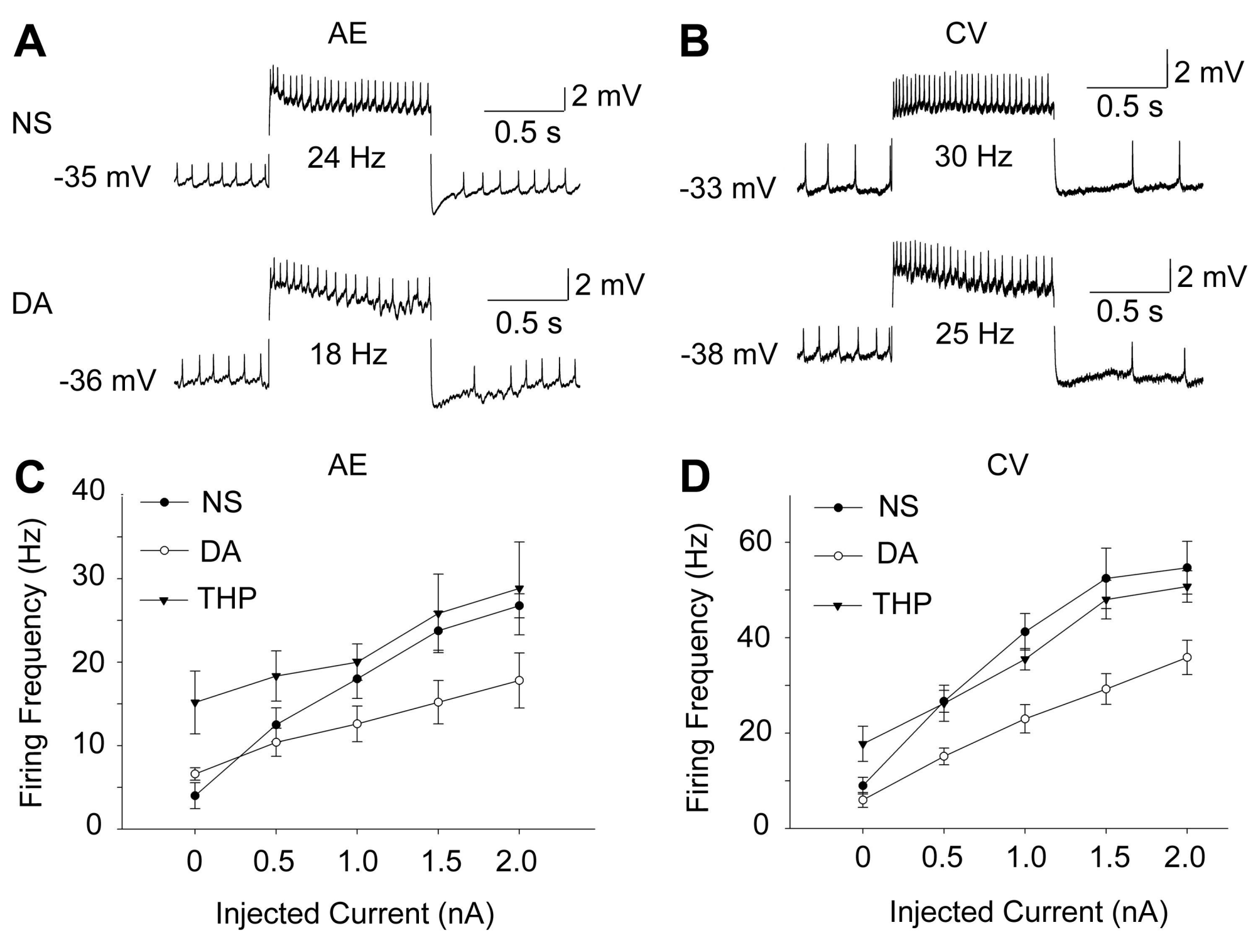
A
AE
NS
-35 mV
24 Hz
2 mV
0.5 s
DA
-36 mV
18 Hz
2 mV
0.5 s
B
CV
-33 mV
30 Hz
2 mV
0.5 s
-38 mV
25 Hz
2 mV
0.5 s
C
AE
NS
DA
THP
Firing Frequency (Hz)
Injected Current (nA)
D
CV
NS
DA
THP
Firing Frequency (Hz)
Injected Current (nA)